

Published in final edited form as:

Ann Neurol. 2009 June ; 65(6): 733–741. doi:10.1002/ana.21678.

A Novel Na_v1.7 Mutation Producing Carbamazepine-Responsive Erythromelalgia

Tanya Z. Fischer, MD, PhD^{1,2,3}, Elaine S. Gilmore, MD, PhD^{2,3,4}, Mark Estacion, PhD^{1,2,3}, Emmanuella Eastman, BS^{1,2,3}, Sean Taylor, MD⁵, Michel Melanson, MD⁵, Sulayman D. Dib-Hajj, PhD^{1,2,3}, and Stephen G. Waxman, MD, PhD^{1,2,3}

¹Department of Neurology, Yale University School of Medicine, New Haven

²Center for Neuroscience & Regeneration Research, Yale University School of Medicine, New Haven

³Rehabilitation Research Center, Veterans Affairs Connecticut Healthcare System, West Haven

⁴Department of Dermatology, Yale University School of Medicine, New Haven, CT

⁵Department of Neurology, Kingston General Hospital, Kingston, Ontario, Canada

Abstract

Objective—Human and animal studies have shown that Na_v1.7 sodium channels, which are preferentially expressed within nociceptors and sympathetic neurons, play a major role in inflammatory and neuropathic pain. Inherited erythromelalgia (IEM) has been linked to gain-of-function mutations of Na_v1.7. We now report a novel mutation (V400M) in a three-generation Canadian family in which pain is relieved by carbamazepine (CBZ).

Methods—We extracted genomic DNA from blood samples of eight members of the family, and the sequence of *SCN9A* coding exons was compared with the reference Na_v1.7 complementary DNA. Wild-type Na_v1.7 and V400M cell lines were then analyzed using whole-cell patch-clamp recording for changes in activation, deactivation, steady-state inactivation, and ramp currents.

Results—Whole-cell patch-clamp studies of V400M demonstrate changes in activation, deactivation, steady-state inactivation, and ramp currents that can produce dorsal root ganglia neuron hyperexcitability that underlies pain in these patients. We show that CBZ, at concentrations in the human therapeutic range, normalizes the voltage dependence of activation and inactivation of this inherited erythromelalgia mutation in Na_v1.7 but does not affect these parameters in wild-type Na_v1.7.

Interpretation—Our results demonstrate a normalizing effect of CBZ on mutant Na_v1.7 channels in this kindred with CBZ-responsive inherited erythromelalgia. The selective effect of CBZ on the mutant Na_v1.7 channel appears to explain the ameliorative response to treatment in

© 2009 American Neurological Association

Address correspondence to Dr Waxman, Department of Neurology, LCI 707, Yale School of Medicine, 333 Cedar Street, New Haven, CT 06510. stephen.waxman@yale.edu.

T.Z.F. and E.S.G. contributed equally to this work.

Potential conflict of interest: Nothing to report.

this kindred. Our results suggest that functional expression and pharmacological studies may provide mechanistic insights into hereditary painful disorders.

Recent studies have confirmed a central role for Na_v1.7 sodium channels in human pain syndromes.^{1,2} Na_v1.7, which is preferentially expressed in nociceptive dorsal root ganglion (DRG) neurons and sympathetic ganglion,^{3–6} is a “threshold channel” that can amplify small depolarizations such as generator potentials.^{7,8} Gain-of-function dominant mutations of Na_v1.7 cause the inherited painful disorders erythromelalgia^{2,9} and paroxysmal extreme pain disorder (PEPD),¹⁰ whereas loss-of-function recessive mutations in Na_v1.7 cause congenital insensitivity to pain.¹¹

Inherited erythromelalgia (IEM) is caused by mutations in Na_v1.7 that produce nociceptive DRG neuron hyperexcitability. Erythromelalgia is characterized by intense burning pain associated with redness of the affected extremities, triggered by mild warmth.^{12,13} Pharmacotherapy for IEM has generally been reported to be ineffective; although controlled studies have not been conducted, the available anecdotal reports in the literature suggest that local anesthetic sodium channel blockers, for example, lidocaine and mexiletine, may provide partial relief in some cases, although they are ineffective in others, and treatment with carbamazepine (CBZ) is usually ineffective.¹⁴ Biophysical analysis of disease-causing mutations provides mechanistic insights and can help predict the efficacy of a particular treatment regimen. For example, some IEM mutations can reduce the channel’s affinity of lidocaine binding,¹⁵ which may explain the refractoriness of some cases to this treatment. In this article, we describe a family with CBZ-responsive IEM, characterize the sodium channel mutation and the physiological changes in channel function produced by this mutation, and show that CBZ normalizes inactivation and activation of these mutant Na_v1.7 channels. Thus, we document an effect of CBZ in IEM, delineate the biophysical basis for this effect, and suggest that *in vitro* characterization of the response of sodium channels to modulators can provide mechanistic insights into chronic pain syndromes.

Subjects and Methods

Exon Screening

Patients were recruited under an approved institutional protocol. Human variation control DNA (69 white male patients and 69 white female patients; Coriell Institute, Camden, NJ) served as control samples. All coding exons and flanking intronic sequences, as well as exons encoding 5′ and 3′ untranslated sequences within the complementary DNA, were amplified and sequenced as described previously.¹⁶ Genomic sequences were compared with the reference Na_v1.7 complementary DNA¹⁷ using the basic local alignment search tool (BLAST; National Library of Medicine, Bethesda, MD) and Lasergene (DNASar, Madison, WI). Sequencing was performed at the Howard Hughes Medical Institute/Keck Biotechnology Center at Yale University (New Haven, CT).

Voltage-Clamp Electrophysiology

The V400M mutation was introduced into a tetrodotoxin (TTX)-resistant version of human Na_v1.7 complementary DNA (hNa_v1.7_R) using QuickChange XL site-directed mutagenesis (Stratagene, La Jolla, CA). Transfected human embryonic kidney (HEK) 293 cells, grown

under standard culture conditions (5% CO₂, 37°C) in Dulbecco's modified Eagle's medium supplemented with 10% fetal bovine serum, were treated with G418 for several weeks to derive stable cell lines that express the mutant or wild-type (WT) channels, as described previously.^{18,19} Use of stable cell lines reduces variability for current density.

Whole-cell voltage-clamp recordings were performed on isolated HEK 293 cells stably expressing WT hNa_v1.7_R or V400M mutant channels at room temperature (approximately 21°C). Electrodes were pulled from 1.6mm outer diameter borosilicate glass micropipettes (WPI, Sarasota, FL) and had a resistance of 1 to 1.5MΩ when filled with pipette solution, which contained (in mM): 140 CsF, 10 NaCl, 10 HEPES, 1 EGTA (pH 7.3 with CsOH, adjusted to 320mOsm with dextrose). The extracellular solution contained (in mM): 140 NaCl, 3 KCl, 1 MgCl₂, 1 CaCl₂, 10 HEPES (pH 7.3 with NaOH, adjusted to 320mOsm with dextrose). Voltage-clamp currents were recorded 3 minutes after establishing whole-cell configuration on an Axopatch 200B amplifier (Molecular Devices, Sunnyvale, CA) and stored via a Digidata 1322a A/D converter (Molecular Devices) at an acquisition rate of 50kHz with a low-pass Bessel filter setting of 5kHz. Voltage errors were minimized with 80 to 95% series resistance compensation, and only cells whose predicted voltage error after compensation was less than 3mV were included for analysis. When appropriate, linear leak currents and capacitance artifacts were subtracted out using the P/N method provided by Clampex (Molecular Devices) acquisition software. Clampfit (Molecular Devices) and Origin (Microcal Software, Northampton, MA) were used for data analysis. Data are expressed as means ± standard error. Statistical significance was determined by Student's *t* test.

For voltage-clamp studies examining response to CBZ treatment, stock solutions of CBZ (Sigma-Aldrich, St. Louis, MO) with a final concentration of 300mM were prepared in DMSO (dimethylsulfoxide). Studies were performed in extracellular solution containing 1% DMSO (control vehicle) or stock concentrations of CBZ prepared freshly in DMSO and then diluted 1:100 in extracellular bath solution to give the indicated final concentrations. The effect of CBZ on the WT and V400M mutant channels was tested from the resting and inactivated states using recordings obtained with the PatchXpress (Molecular Devices, Union City, CA) automated patch-clamp system. For blocking from the resting state, the following protocol was used: Cells were held at -120mV in the presence of DMSO (control vehicle) or CBZ and then stepped through potentials from -80 to +60mV, in 10mV increments for 100 milliseconds. For blocking from the inactivated state, the voltage-clamp protocol was as follows: Cells were held at -50mV for 10 seconds to inactivate the Na_v1.7 channels in the presence of vehicle (DMSO) or CBZ in the bath solution; the cells were pulsed to -120mV for 100 milliseconds to allow channels not bound by drug to recover from fast inactivation and then given a 20-millisecond test pulse to 0mV to measure available currents. Cells were normalized to the currents elicited from the same protocols applied just before compound addition, and data expressed as fraction of current remaining. The IC₅₀ (50% of inhibitory concentration) of CBZ for WT and V400M mutant channels were obtained by fitting the dose-response curves. Where indicated, data were analyzed using univariate analysis of variance methods, followed by Tukey's honestly significant differences test.

Results

Clinical Studies

The proband is a 37-year-old man who presented to his physician with a lifelong history of episodic erythema and burning pain in both feet. His symptoms began before the age of 1 year. The episodes of pain and erythema last for approximately 20 minutes and are triggered by warmth and exercise. The patient prefers wearing open-toed shoes without socks, even during the winter months. Interestingly, treatment with 800mg/day CBZ provided significant pain relief for the patient. The proband's mother, two children, and brother have similar symptoms. The proband's two children also experienced nearly total pain relief within 3 days of starting 400mg/day CBZ (Fig 1). One child had approximately 56 attacks per week before starting CBZ, but while on medication, he has about 2 attacks per week. The other child has had a similar response. Before treatment with CBZ, the children cooled their feet with a fan at night, could not tolerate wearing socks or shoes, and could not participate in athletics; however, since starting this medication, they do not require a fan blowing on their feet at night, and are both able to run, play soccer, and wear socks and shoes.

Identification of V400M Mutation in Exon 9

Sequence analysis of *SCN9A* amplicons identified a nucleotide change (1198 G>A) in exon 9, which causes a substitution of valine at position 400 of the reference $\text{Na}_v1.7$ sequence¹⁷ by methionine (V400M). V400 is located near the C terminus of transmembrane segment 6 in domain I (DI/S6), a segment that is located close to the channel pore; the V400M residue is invariant in all of the mammalian voltage-gated sodium channels. The mutation segregates with the affected members in this family but not in the unaffected family members (see Fig 1) and was not present in 276 ethnically matched control alleles.

V400M Shifts Voltage Dependence of Activation

The effects of the V400M mutation on $\text{Na}_v1.7$ channel function (Table 1) were studied in a HEK 293 cell line stably producing these channels. Activation curves were generated by holding cells at -120mV and then stepping through potentials from -80 to $+60\text{mV}$, in 10mV increments for 100 milliseconds. Representative traces for both WT and V400M mutant channels are shown in Figures 2A and B. Normalized current-voltage (I/V) curves show a hyperpolarizing shift in activation for the V400M mutant channels (see Fig 2C). Boltzmann fits of activation curves normalized to maximal conductance (see Fig 2D) demonstrate a significant ($p < 0.01$) 6.5mV hyperpolarizing shift in activation of mutant channels (WT: $V_{1/2} = -43.9 \pm 1.47\text{mV}$; $n = 15$; V400M: $V_{1/2} = -50.4 \pm 1.64\text{mV}$; $n = 18$). There was no statistical difference in the slope factor (k) for these curves (WT: $k = 4.30 \pm 0.455$; V400M: $k = 4.11 \pm 0.365$).

V400M Shifts Voltage Dependence of Steady-State Inactivation

Steady-state fast inactivation was tested by stepping cells from a prepulse holding potential (-130 to -10mV ; 500 milliseconds) to a test potential of -10mV for 100 milliseconds. Figure 3A shows Boltzmann fits of steady-state fast-inactivation curves normalized to maximum current and demonstrates a significant ($p < 0.001$) depolarizing shift (7.3mV) in

fast inactivation for cells expressing the V400M as compared with WT channels (WT: $V_{1/2} = -90.1 \pm 1.44\text{mV}$; V400M: $V_{1/2} = -82.8 \pm 1.44\text{mV}$). The 7.3mV depolarizing shift in $V_{1/2}$ for steady-state fast inactivation, in conjunction with the 6.5mV hyperpolarizing shift in activation for V400M mutants, together significantly increase the overlap window current for the channel (see Figs 3B, C). Analyses of the kinetics of fast inactivation (τ) (see Fig 3D) demonstrated no differences in this parameter between cells expressing the V400M mutant versus WT channels.

V400M Slows Deactivation

Current decay time constants (τ) were measured at 10mV increments for potentials from -100 to -40mV after a short depolarizing step to 0mV for 0.5 millisecond. Voltage-dependent deactivation curves for cells expressing V400M versus WT channels (see Fig 3E) show a statistically significant, progressive slowing of deactivation for mutant channels (** $p < 0.0005$; * $p < 0.005$; ++ $p < 0.02$; + $p < 0.05$).

To measure the voltage dependence of steady-state slow inactivation, we pulsed cells for 30 seconds to potentials ranging from -120 to $+10\text{mV}$ followed by a 100-millisecond hyperpolarizing pulse to -120mV to remove fast inactivation before stepping to the depolarizing test potential of 0mV . Boltzmann fits of normalized current-voltage curves (see Fig 3F) generated from this protocol demonstrated no significant difference between WT and V400M mutant channels (WT: $V_{1/2} = -73.9 \pm 3.9\text{mV}$, $n = 16$; V400M: $V_{1/2} = -76.2 \pm 3.9\text{mV}$, $n = 18$). In addition, there was no significant difference in the slope factor (k) for these curves (WT: $k = 12.4 \pm 1.9$; V400M: $k = 13.1 \pm 2.7$).

V400M Enhances Responses to Ramp Stimuli

The response of the V400M mutation to slow ramp depolarizations was assessed by depolarizing cells held at -120 to 20mV over a 600-millisecond time course ($0.23\text{mV}/\text{msec}$). Results depicted in Figure 4 show a twofold increase in the inward current in cells expressing the V400M mutant channels ($1.81 \pm 0.22\%$ of peak current; $n = 7$) as compared with WT channels ($0.945 \pm 0.114\%$ of peak current; $n = 12$). In addition, the voltage of peak inward currents during the slow-ramp depolarization was significantly shifted in the hyperpolarizing direction ($p < 0.02$) for cells expressing V400M mutant channels ($-63.1 \pm 2.36\text{mV}$; $n = 7$) as compared with WT channels ($-54.2 \pm 1.05\text{mV}$; $n = 12$).

Resting- and Inactivated-State Block of V400M Channels by Carbamazepine

Given the unique ameliorative effect of CBZ in this kindred with erythromelalgia, we examined the effect of CBZ on the biophysical properties of the V400M mutant channels. The resting-state block of WT and V400M mutant channels was evaluated by comparing the response to a 0mV test pulse from a holding potential of -120mV recorded before and after application of concentrations of CBZ ranging from $3\mu\text{M}$ to 1mM (Fig 5A). Logistic fits of the data indicate that the IC_{50} for WT channels is $1,350\mu\text{M}$, and the IC_{50} for V400M channels is $970\mu\text{M}$.

CBZ is a known state-dependent channel blocker; thus, we evaluated the blocking effect of CBZ on the inactivated state of the WT and V400M mutant channels. Cells were prepulsed

to -50mV for 10 seconds to induce fast inactivation in the presence of CBZ in the bath solution, followed by a hyperpolarizing pulse to -120mV to allow channels not bound with drug to recover from inactivation; then the remaining current was assessed with a 0mV test pulse for 20 milliseconds. The recorded current was normalized to the response recorded in the same cell just before adding CBZ (see Fig 5B). Logistic fits of the data indicate that the IC_{50} for inactivated WT channels is $1,100\mu\text{M}$, and the IC_{50} for inactivated V400M channels is $1,030\mu\text{M}$.

Carbamazepine Normalizes Activation in V400M Channels

The voltage dependence of activation and steady-state fast inactivation were measured in HEK 293 cells stably expressing the WT or V400M mutant channels in the presence of 1% DMSO (control), $10\mu\text{M}$ CBZ, or $100\mu\text{M}$ CBZ (Table 2). These concentrations of CBZ were selected because they are similar to concentrations achieved during effective prevention of electroconvulsive shock-induced seizures²⁰ and therapeutic serum concentrations in treated patients.²¹ Figure 6A shows effects of CBZ on activation in cells producing the V400M mutant channels, with depolarizing shifts in the activation curve in response to CBZ application (V400M: $V_{1/2 \text{ DMSO}} = -47.9 \pm 2.9\text{mV}$; $V_{1/2 10\mu\text{M CBZ}} = -36.9 \pm 1.2\text{mV}$; $V_{1/2 100\mu\text{M CBZ}} = -37.3 \pm 2.7\text{mV}$). Interestingly, the shift in activation did not change on increasing the CBZ concentration 10-fold. The shift in activation with $10\mu\text{M}$ CBZ produces a curve that coincides with that for activation of WT channels (WT: $V_{1/2 \text{ DMSO}} = -36.6 \pm 2.6\text{mV}$). Notably, treatment with CBZ did not produce any significant shifts in activation of WT channels (see Fig 6B). Because the shift in the voltage dependence of activation is the strongest contributor to the hypersensitivity of DRG neurons having IEM mutations,¹⁵ we determined the EC_{50} (50% of effective concentration) for the effect of CBZ treatment on the activation voltage dependence of V400M mutant channels. For these experiments, additional lower concentrations of CBZ were tested, and the average activation $V_{1/2}$ was plotted as a function of CBZ concentration (see Fig 6E). The logistic fit to these data indicate an EC_{50} of $3.4\mu\text{M}$ with a Hill coefficient of 3.7.

Carbamazepine Normalizes Inactivation in V400M Channels

CBZ treatment produced hyperpolarizing shifts in steady-state fast inactivation in cells expressing the V400M mutation but not WT channels (V400M: $V_{1/2 \text{ DMSO}} = -87.2 \pm 2\text{mV}$; $V_{1/2 10\mu\text{M CBZ}} = -91.7 \pm 1.5\text{mV}$; $V_{1/2 100\mu\text{M CBZ}} = -92.9 \pm 2.7\text{mV}$). As shown in Figure 6C, increasing concentrations of CBZ produced a hyperpolarizing shift in the fast-inactivation curve, which was shifted to coincide with that of WT channels (WT: $V_{1/2 \text{ DMSO}} = -93.1 \pm 3.3\text{mV}$). CBZ is known to produce shifts in fast inactivation of WT channels at greater concentrations (1mM)²² than were used in these studies. Treatment with 10 or $100\mu\text{M}$ CBZ did not affect the voltage dependence of fast inactivation of WT channels (see Fig 6D).

Discussion

We have described a family with IEM in which pain was effectively relieved with CBZ, a treatment previously reported as ineffective for this pain disorder, and have characterized a new $\text{Na}_v1.7$ sodium channel mutation (V400M) within the DI/S6 transmembrane segment, located close to the channel intracellular pore, which is linked to IEM in this family. We

demonstrate a V400M-induced hyperpolarizing shift in the voltage dependence of activation, a slowing of kinetics of deactivation, a depolarizing shift in voltage dependence of fast inactivation, and an increase in inward currents in response to a slow-voltage ramp. Computer simulations suggest that changes in the voltage dependence of activation constitute the major contributor to DRG neuron hyperexcitability in IEM.¹⁵ We show that CBZ at concentrations within the therapeutic range normalizes the effect of V400M mutation on channel activation. Thus, our data link biophysical changes in the V400M mutation of Na_v1.7 to pain in these IEM patients and provide mechanistic basis for the ameliorative effect of CBZ in these patients.

The finding that several members of this kindred respond nearly completely to treatment with CBZ is unique among patients with IEM. Traditionally, CBZ has been used to reduce neuronal excitability, particularly in epilepsy and trigeminal neuralgia. CBZ is a state-dependent sodium channel blocker, preferentially binding to sodium channels in the inactivated state to produce a negative shift in steady-state fast inactivation.^{23–25} In practice, a therapeutic response to CBZ has not been described previously in IEM, and CBZ has been found to be more useful for control of symptoms in patients with another distinct painful neuropathy: PEPD.¹⁰ Sodium channels expressing PEPD mutations display impaired fast inactivation and a persistent current that is attenuated by CBZ¹⁰; thus, successful use of CBZ, as observed clinically, in the PEPD patient population is predicted. In this article, we describe a kindred with IEM that responds favorably to CBZ and show that CBZ, at clinically relevant concentrations that bind to and block sodium channels and inhibit shock-induced seizures,²⁰ normalizes fast inactivation of the mutant Na_v1.7 channel, shifting the hyperpolarized voltage dependence of its inactivation back to WT values. Surprisingly, we also observed that CBZ normalized activation in V400M mutant channels, shifting their voltage dependence toward WT values. These depolarizing shifts were seen only in mutant channels and not in WT channels, at concentrations that are much lower than needed to block either WT or V400M mutant channels. This predicts a useful range of CBZ concentrations that may promote a therapeutic effect by normalizing the function of V400M mutant Na_v1.7 channels without blocking either the mutant or the WT Na_v1.7 channels.

The V400M mutation within the D1/S6 segment of Na_v1.7 is located in proximity to the local anesthetic binding pocket of the channel. A mutation causing a single amino acid substitution at the K354 residue in Na_v1.3, located within the pore region immediately proximal to D1/S6, has been linked to CBZ-resistant epilepsy, a finding that caused the authors to suggest that sensitivity to CBZ may be modulated by the configuration of this part of the channel.²⁶ Pharmacological observations indicate that the anticonvulsant receptor responsible for block of sodium channels by CBZ, located within the channel pore, changes its configuration to alter drug binding and blocking action, depending on the channel's gating state.²⁷ We speculate that the location of the V400M mutation in the D1/S6 of Na_v1.7, which is close to the local anesthetic binding region, contributes both to the altered voltage dependence of the mutant channel and to its sensitivity to CBZ.

Interestingly, an identical mutation at the corresponding site in Na_v1.4 (V445M) has been shown to underlie several cases of painful congenital myotonia,^{28,29} including patients who respond favorably to mexiletine.²⁹ It has been shown that the V445M mutation increases by

twofold the affinity of mexiletine to inactivated mutant $\text{Na}_v1.4$ channels,³⁰ which may explain the favorable response to the drug. Unlike the V445M mutation in $\text{Na}_v1.4$, the effect of CBZ on the V400M mutation in $\text{Na}_v1.7$ appears to be mediated by a different mechanism that affects voltage dependence of activation rather than frequency-dependent block. Whether the different modes of action reflect isoformspecific differences or drug-specific effects is not known.

In summary, we report a family with CBZ-responsive IEM, and using functional analysis, we demonstrate a normalizing effect of CBZ on the physiological properties of the mutant $\text{Na}_v1.7$ channel. Given the strong contribution of peripheral neuron-specific sodium channels such as $\text{Na}_v1.7$ to pain^{1,31} and the presence of polymorphisms, as well as mutations in sodium channel genes, functional expression studies are likely to yield new insights into familial pain syndromes and may identify novel mechanisms for normalization of function of mutant ion channels.

Acknowledgments

This work was supported by the Medical Research Service and Rehabilitation Research Service, Department of Veterans Affairs (S.G.W.), and the National Multiple Sclerosis Society (RG-1912; S.G.W.) and the Erythromelalgia Association (S.G.W.). The Center for Neuroscience and Regeneration Research is a Collaboration of the Paralyzed Veterans of America and the United Spinal Association with Yale University.

We thank L. Tyrrell, J. Sung Choi, X. Cheng, L. Macala, B. Toftness, and L. Marshall for excellent technical assistance. We thank J. Ryan for assistance with statistics.

References

1. Waxman SG. Neurobiology: a channel sets the gain on pain. *Nature*. 2006; 444:831–832. [PubMed: 17167466]
2. Dib-Hajj SD, Cummins TR, Black JA, Waxman SG. From genes to pain: Nav 1.7 and human pain disorders. *Trends Neurosci*. 2007; 30:555–563. [PubMed: 17950472]
3. Djouhri L, Newton R, Levinson SR, et al. Sensory and electrophysiological properties of guinea-pig sensory neurones expressing Nav 1.7 (PN1) Na⁺ channel alpha subunit protein. *J Physiol*. 2003; 546:565–576. [PubMed: 12527742]
4. Black JA, Dib-Hajj S, McNabola K, et al. Spinal sensory neurons express multiple sodium channel alpha-subunit mRNAs. *Brain Res Mol Brain Res*. 1996; 43:117–131. [PubMed: 9037525]
5. Sangameswaran L, Fish LM, Koch BD, et al. A novel tetrodotoxin-sensitive, voltage-gated sodium channel expressed in rat and human dorsal root ganglia. *J Biol Chem*. 1997; 272:14805–14809. [PubMed: 9169448]
6. Toledo-Aral JJ, Moss BL, He ZJ, et al. Identification of PN1, a predominant voltage-dependent sodium channel expressed principally in peripheral neurons. *Proc Natl Acad Sci U S A*. 1997; 94:1527–1532. [PubMed: 9037087]
7. Cummins TR, Howe JR, Waxman SG. Slow closed-state inactivation: a novel mechanism underlying ramp currents in cells expressing the hNE/PN1 sodium channel. *J Neurosci*. 1998; 18:9607–9619. [PubMed: 9822722]
8. Rush AM, Cummins TR, Waxman SG. Multiple sodium channels and their roles in electrogenesis within dorsal root ganglion neurons. *J Physiol*. 2007; 579:1–14. [PubMed: 17158175]
9. Waxman SG, Dib-Hajj S. Erythromelalgia: molecular basis for an inherited pain syndrome. *Trends Mol Med*. 2005; 11:555–562. [PubMed: 16278094]
10. Fertleman CR, Baker MD, Parker KA, et al. SCN9A mutations in paroxysmal extreme pain disorder: allelic variants underlie distinct channel defects and phenotypes. *Neuron*. 2006; 52:767–774. [PubMed: 17145499]

11. Cox JJ, Reimann F, Nicholas AK, et al. An SCN9A channelopathy causes congenital inability to experience pain. *Nature*. 2006; 444:894–898. [PubMed: 17167479]
12. van Genderen PJ, Michiels JJ, Drenth JP. Hereditary erythralgia and acquired erythromelalgia. *Am J Med Genet*. 1993; 45:530–532. [PubMed: 8465864]
13. Novella SP, Hisama FM, Dib-Hajj SD, Waxman SG. A case of inherited erythromelalgia. *Nat Clin Pract Neurol*. 2007; 3:229–234. [PubMed: 17410110]
14. Drenth JP, Waxman SG. Mutations in sodium-channel gene SCN9A cause a spectrum of human genetic pain disorders. *J Clin Invest*. 2007; 117:3603–3609. [PubMed: 18060017]
15. Sheets PL, Jackson JO 2nd, Waxman SG, et al. A Nav1.7 channel mutation associated with hereditary erythromelalgia contributes to neuronal hyperexcitability and displays reduced lidocaine sensitivity. *J Physiol*. 2007; 581:1019–1031. [PubMed: 17430993]
16. Dib-Hajj SD, Rush AM, Cummins TR, et al. Gain-of-function mutation in Nav1.7 in familial erythromelalgia induces bursting of sensory neurons. *Brain*. 2005; 128:1847–1854. [PubMed: 15958509]
17. Klugbauer N, Lacinova L, Flockerzi V, Hofmann F. Structure and functional expression of a new member of the tetrodotoxin-sensitive voltage-activated sodium channel family from human neuroendocrine cells. *EMBO J*. 1995; 14:1084–1090. [PubMed: 7720699]
18. Han C, Rush AM, Dib-Hajj SD, et al. Sporadic onset of erythromelalgia: a gain-of-function mutation in Nav1.7. *Ann Neurol*. 2006; 59:553–558. [PubMed: 16392115]
19. Lampert A, Dib-Hajj SD, Tyrrell L, Waxman SG. Size matters: erythromelalgia mutation S241T in Nav1.7 alters channel gating. *J Biol Chem*. 2006; 281:36029–36035. [PubMed: 17008310]
20. Willow M, Gonoi T, Catterall WA. Voltage clamp analysis of the inhibitory actions of diphenylhydantoin and carbamazepine on voltage-sensitive sodium channels in neuroblastoma cells. *Mol Pharmacol*. 1985; 27:549–558. [PubMed: 2581124]
21. Breton H, Cociglio M, Bressolle F, et al. Liquid chromatography-electrospray mass spectrometry determination of carbamazepine, oxcarbazepine and eight of their metabolites in human plasma. *J Chromatogr B Analyt Technol Biomed Life Sci*. 2005; 828:80–90.
22. Sheets PL, Heers C, Stoehr T, Cummins TR. Differential block of sensory neuronal voltage-gated sodium channels by lacosamide [(2R)-2-(acetylamino)-N-benzyl-3-methoxypropanamide], lidocaine, and carbamazepine. *J Pharmacol Exp Ther*. 2008; 326:89–99. [PubMed: 18378801]
23. Backus KH, Pflimlin P, Trube G. Action of diazepam on the voltage-dependent Na⁺ current. Comparison with the effects of phenytoin, carbamazepine, lidocaine and flumazenil. *Brain Res*. 1991; 548:41–49. [PubMed: 1651146]
24. Ragsdale DS, Scheuer T, Catterall WA. Frequency and voltage-dependent inhibition of type IIA Na⁺ channels, expressed in a mammalian cell line, by local anesthetic, antiarrhythmic, and anticonvulsant drugs. *Mol Pharmacol*. 1991; 40:756–765. [PubMed: 1658608]
25. Song JH, Nagata K, Huang CS, et al. Differential block of two types of sodium channels by anticonvulsants. *Neuroreport*. 1996; 7:3031–3036. [PubMed: 9116234]
26. Holland KD, Kearney JA, Glauser TA, et al. Mutation of sodium channel SCN3A in a patient with cryptogenic pediatric partial epilepsy. *Neurosci Lett*. 2008; 433:65–70. [PubMed: 18242854]
27. Yang YC, Kuo CC. Inhibition of Na⁽⁺⁾ current by imipramine and related compounds: different binding kinetics as an inactivation stabilizer and as an open channel blocker. *Mol Pharmacol*. 2002; 62:1228–1237. [PubMed: 12391287]
28. Rosenfeld J, Sloan-Brown K, George AL Jr. A novel muscle sodium channel mutation causes painful congenital myotonia. *Ann Neurol*. 1997; 42:811–814. [PubMed: 9392583]
29. Trip J, Faber CG, Ginjaar HB, et al. Warm-up phenomenon in myotonia associated with the V445M sodium channel mutation. *J Neurol*. 2007; 254:257–258. [PubMed: 17334961]
30. Takahashi MP, Cannon SC. Mexiletine block of disease-associated mutations in S6 segments of the human skeletal muscle Na⁽⁺⁾ channel. *J Physiol*. 2001; 537:701–714. [PubMed: 11744749]
31. Cummins TR, Sheets PL, Waxman SG. The roles of sodium channels in nociception: Implications for mechanisms of pain. *Pain*. 2007; 131:243–257. [PubMed: 17766042]

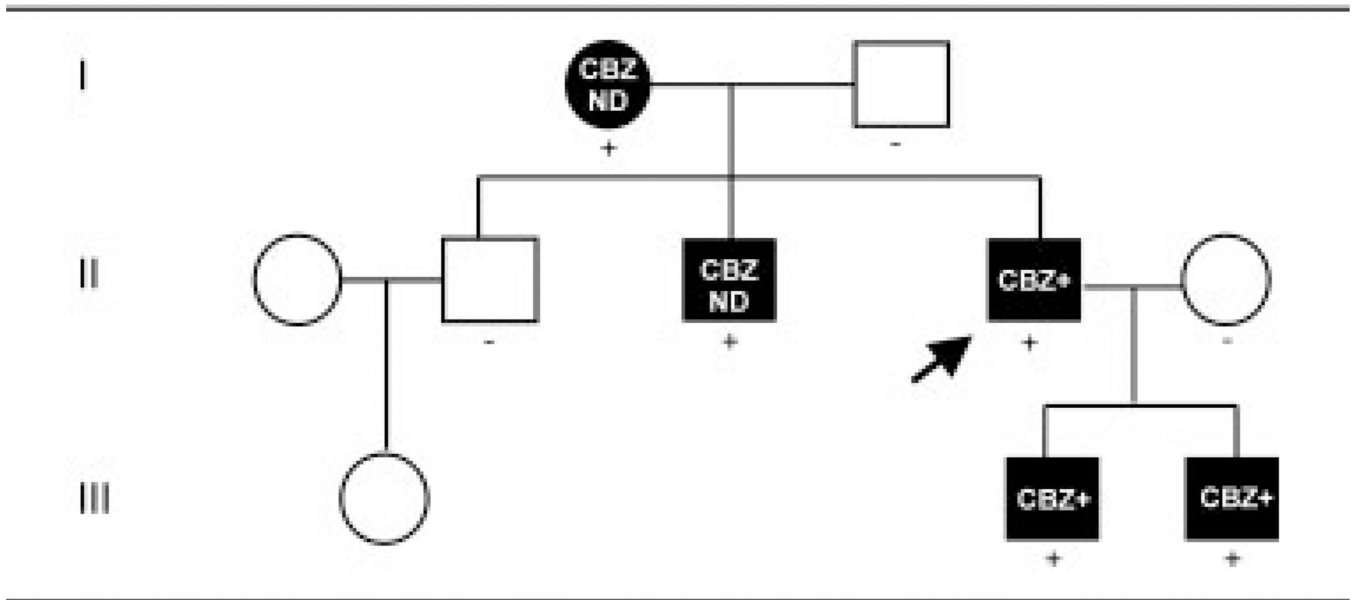


Fig 1. Inheritance pattern of the V400M mutation in $Na_v1.7$ associated with carbamazepine (CBZ)-responsive inherited erythromelalgia (IEM). A three-generation Canadian family with the affected patients all having similar symptoms; the proband is indicated by an *arrow*. *Circles* denote female subjects; *squares* denote male subjects; *black symbols* indicate subjects affected with inherited erythromelalgia; *plus signs* denote subjects heterozygous for the V400M mutation in exon 9; and *minus sign* denotes subjects without the mutation. CBZ+ = pain relief from CBZ treatment; CBZ ND = the effect of CBZ on the patient's symptoms is unknown.

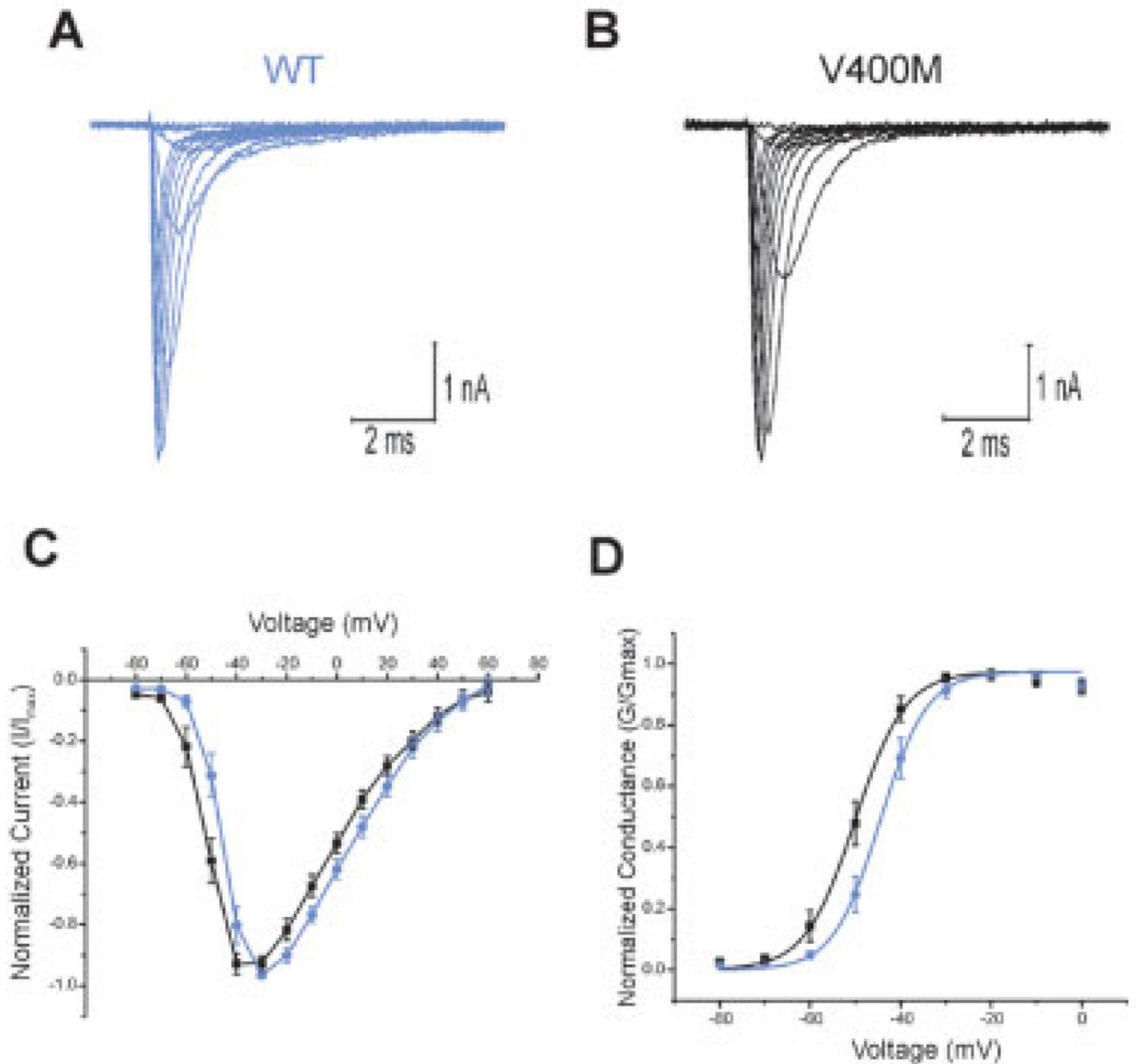


Fig 2. V400M mutation shifts activation. (A, B) Representative traces from human embryonic kidney (HEK) 293 cells stably expressing wild-type (WT; A) and V400M (B) mutant Na_v1.7 channels resulting from voltage steps for generation of activation curves as described in Subjects and Methods. (C) Normalized current-voltage relations generated from activation curves from cells expressing V400M (n = 18; *black squares*) or WT (n = 15; *blue circles*) Na_v1.7 channels. (D) Voltage-dependent hyperpolarizing shift in activation is demonstrated by Boltzmann fits of activation curves from cells expressing V400M (n = 18)

or WT (n = 15) Na_v1.7 channels (V400M: V_{1/2} = -50.4 ± 1.64mV; WT: V_{1/2} = -43.9 ± 1.47mV; *p* < 0.01).

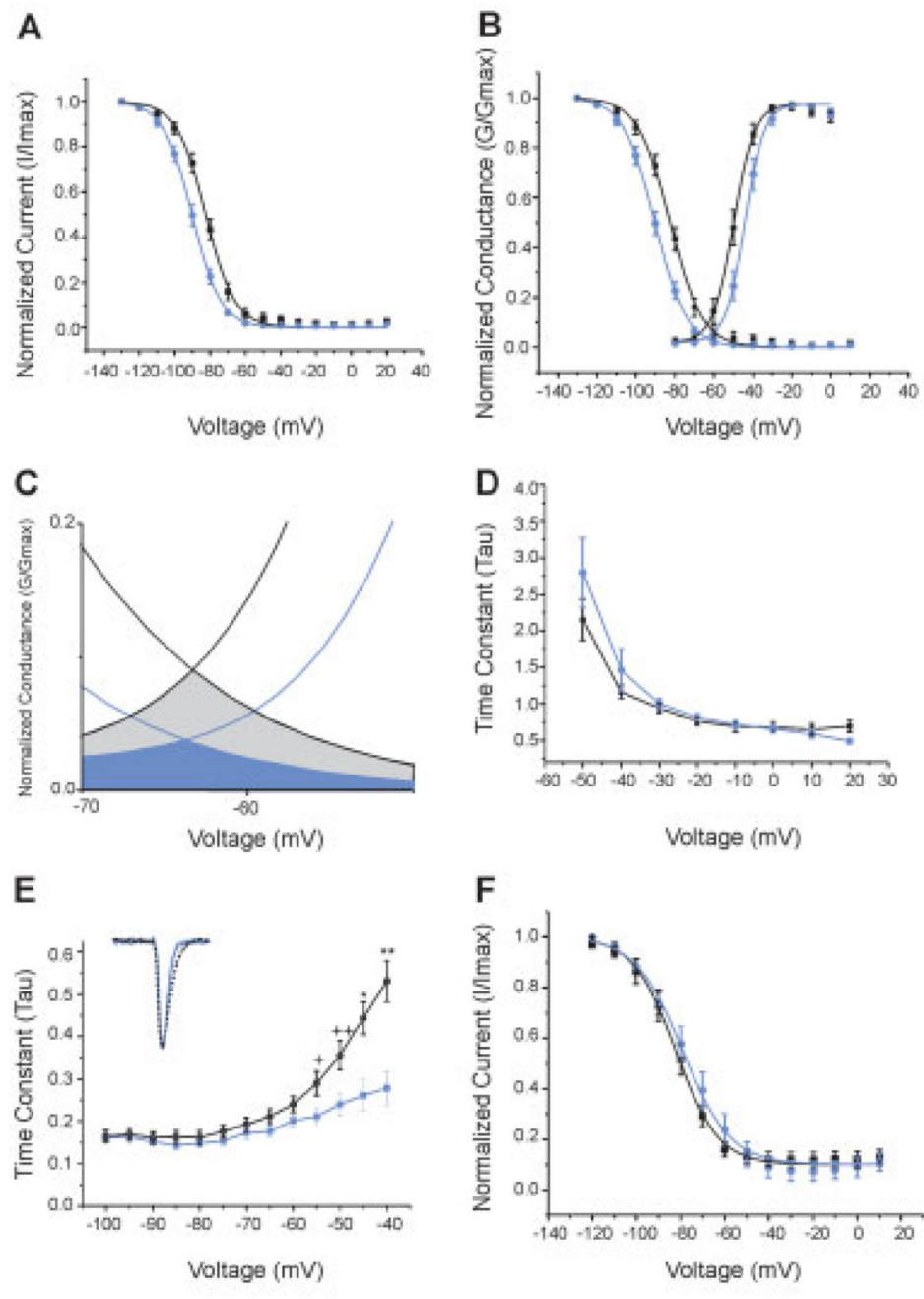


Fig 3. Further characterization of the V400M mutation. (A) Voltage dependence of steady-state inactivation shows a depolarizing shift in cells expressing V400M mutants ($n = 19$; *black squares*) as compared with wild-type (WT) channels ($n = 25$; *blue circles*) (V400M: $V_{1/2} = -82.8 \pm 1.44\text{mV}$; WT: $V_{1/2} = -90.1 \pm 1.44\text{mV}$; $p < 0.001$). (B) Composite graph showing Boltzmann fits of activation and steady-state inactivation curves of V400M mutant versus WT channels shows an increase in overlap window current (enlarged in C: blue represents WT and black represent V400M). (D) Kinetics of fast inactivation as measured by fits of the

time constant (τ) are unchanged in cells expressing V400M mutants ($n = 18$; *black squares*) versus WT ($n = 15$; *blue circles*) channels (not significant). (E) Progressive slowing of the deactivation time constant (τ) is observed in cells expressing V400M mutant channels ($n = 20$) compared with WT channels ($n = 24$) (** $p < 0.0005$; * $p < 0.005$; ++ $p < 0.02$; + $p < 0.05$). (inset) Representative currents and prolonged deactivation at -50mV . *Blue solid line* represents 1.7R WT; *black dashed line* represents 1.7R V400M. (F) Voltage dependence of slow inactivation is unchanged in cells expressing V400M mutant channels ($n = 18$; *black squares*) versus WT channels ($n = 16$; *blue circles*) (V400M: $V_{1/2} = -76.2 \pm 3.9\text{mV}$; WT: $V_{1/2} = 73.9 \pm 3.9\text{mV}$; p value is not significant).

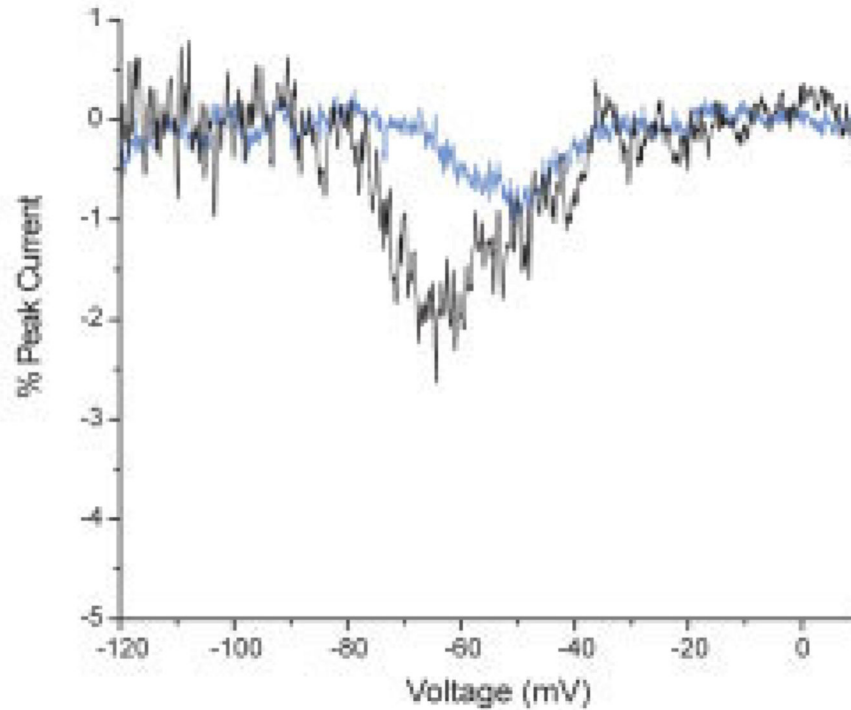
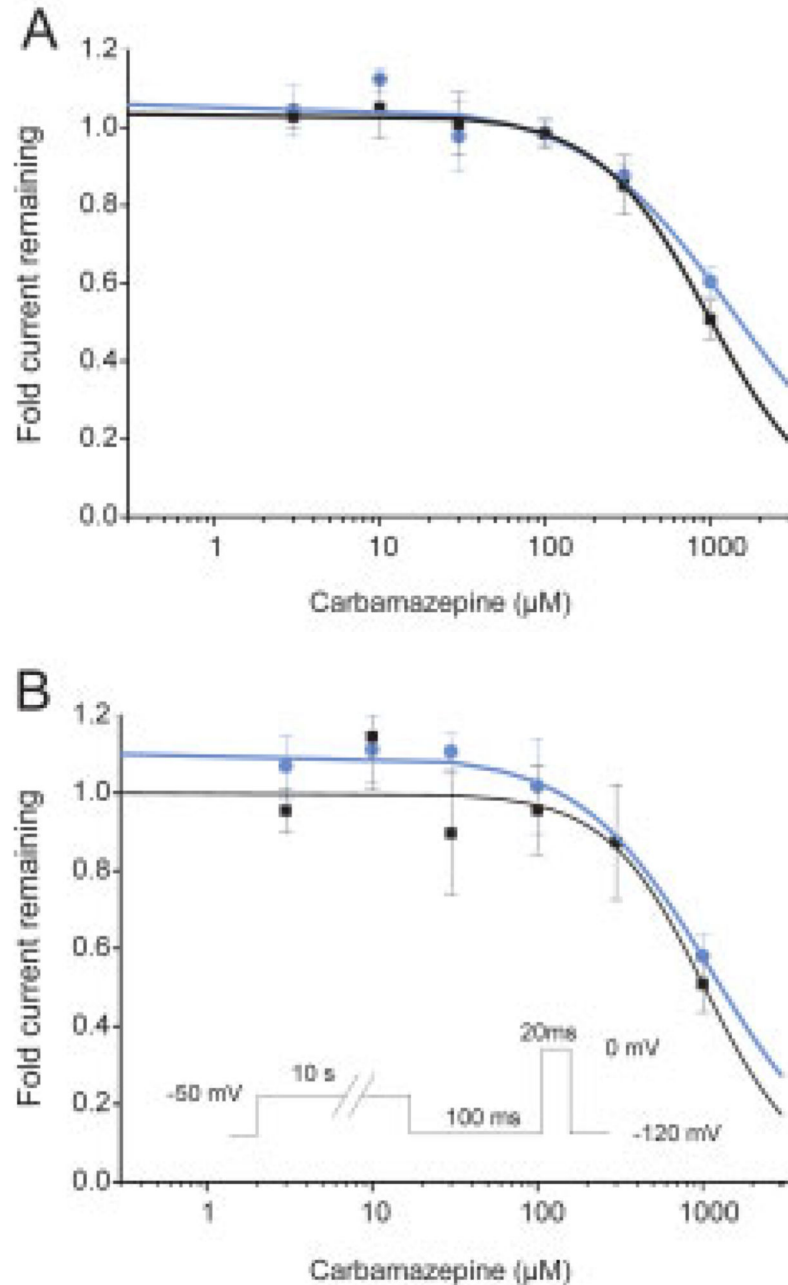


Fig 4. Response to slow-voltage-ramp currents was assessed in human embryonic kidney (HEK) cells expressing V400M mutant channels (*black line*) or wild-type (WT; *blue line*) channels. Shown are representative traces of inward currents (expressed as percentage of peak current obtained with the activation protocol) in response to slow-voltage depolarization from -120 to 20 mV over a 600-millisecond time course (0.23 mV/msec).

**Fig 5.**

Block of wild-type (WT) and V400M mutant Na currents by carbamazepine (CBZ). (A) The holding potential was set to -120mV to maintain the channels in the resting (closed) state; then the current available for activation was elicited by a 20-millisecond pulse to 0mV . The fractional block is given by dividing the current measured in the presence of the indicated concentration of CBZ by the current elicited in the same cell just before compound addition. The IC_{50} fitted to the WT data (blue circles) is $1,350 \pm 230\mu\text{M}$ (adjusted $R^2 = 0.98$). The IC_{50} fitted to the V400M data (black squares) is $970 \pm 30\mu\text{M}$ (adjusted $R^2 = 0.99$). (B) To

evaluate block of inactivated Na channels, we applied a 10-second conditioning pulse to -50mV followed by a 100-millisecond pulse to -120mV to recover from fast inactivation; then the test pulse to 0mV was applied. The IC_{50} fitted to the WT data (*blue circles*) is $1,100 \pm 80\mu\text{M}$ (adjusted $R^2 = 0.98$). The IC_{50} fitted to the V400M data (*black squares*) is $1,030 \pm 160\mu\text{M}$ (adjusted $R^2 = 0.89$).

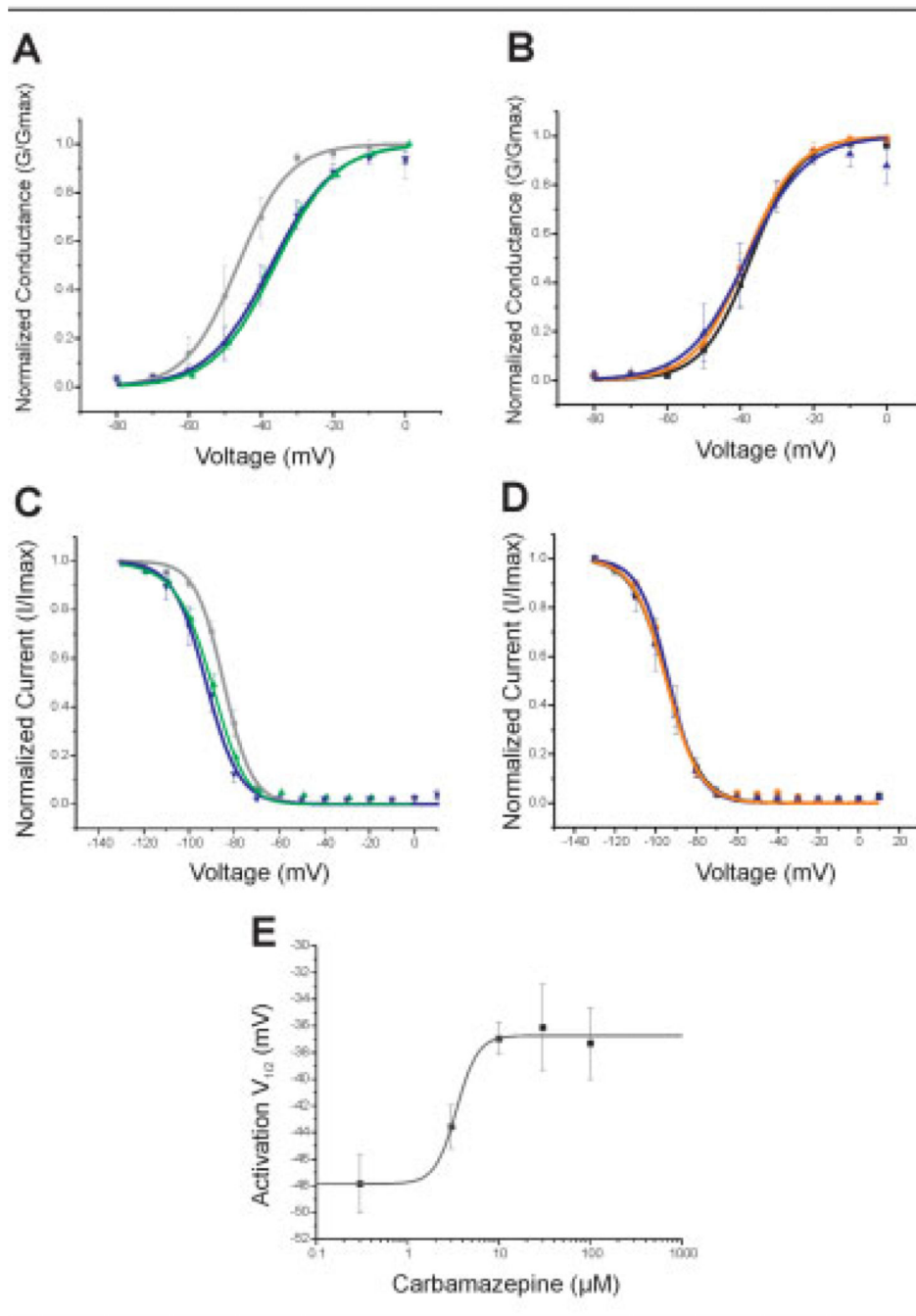


Fig 6. Carbamazepine (CBZ) normalizes the gating properties of the V400M mutation. (A) Depolarizing shifts in the voltage dependence of activation are observed in human embryonic kidney (HEK) 293 cells stably expressing the V400M mutation in response to increasing concentrations of CBZ ($V_{1/2}$ DMSO = -47.9 ± 2.93 mV; $V_{1/2}$ 10 μ M CBZ = -36.9 ± 1.2 mV; $V_{1/2}$ 100 μ M CBZ = -37.3 ± 2.72 mV). *Black circles* designate V400M + DMSO (n = 6); *green upward triangles* designate V400M + 10 μ M CBZ (n = 19); *blue downward triangles* designate V400M + 100 μ M CBZ (n = 8). (B) CBZ treatment of HEK 293 cells

expressing wild-type channels does not affect the voltage dependence of activation ($V_{1/2 \text{ DMSO}} = -36.6 \pm 2.63 \text{ mV}$; $V_{1/2 \text{ } 10 \mu\text{M CBZ}} = -37.9 \pm 1.7 \text{ mV}$; $V_{1/2 \text{ } 100 \mu\text{M CBZ}} = -40.5 \pm 3.28 \text{ mV}$). *Black squares* designate WT + DMSO (n = 9); *orange circles* designate WT + 10 μM CBZ (n = 10); *blue upward triangles* designate V400M + 100 μM CBZ (n = 7). (C) Hyperpolarizing shifts in the voltage dependence of steady-state fast inactivation are observed with CBZ treatment of V400M-expressing cells ($V_{1/2 \text{ DMSO}} = -87.2 \pm 1.97 \text{ mV}$; $V_{1/2 \text{ } 10 \mu\text{M CBZ}} = -91.7 \pm 1.5 \text{ mV}$; $V_{1/2 \text{ } 100 \mu\text{M CBZ}} = -92.9 \pm 2.65 \text{ mV}$). *Black circles* designate V400M + DMSO (n = 8); *green upward triangles* designate V400M + 10 μM CBZ (n = 19); *blue downward triangles* designate V400M + 100 μM CBZ (n = 8). (D) Voltage dependence of steady-state fast inactivation is unchanged by CBZ treatment of cells expressing wild-type channels ($V_{1/2 \text{ DMSO}} = -93.1 \pm 3.32 \text{ mV}$; $V_{1/2 \text{ } 10 \mu\text{M CBZ}} = -94.1 \pm 0.76 \text{ mV}$; $V_{1/2 \text{ } 100 \mu\text{M CBZ}} = -94.7 \pm 1.63 \text{ mV}$). *Black squares* designate WT + DMSO (n = 5); *orange circles* designate WT + 10 μM CBZ (n = 9); *blue upward triangles* designate V400M + 100 μM CBZ (n = 8). (E) The concentration–response curve for the CBZ-induced shifts of the $V_{1/2}$ of activation is plotted for a range of CBZ pretreatment concentrations. Data points are the averages of the activation $V_{1/2}$ values obtained by fitting a Boltzmann function to the GV (conductance-voltage) curves (n = 5–19). A logistic fit of the data suggests that the EC_{50} for CBZ to normalize the $V_{1/2}$ of V400M toward the WT value is $3.4 \pm 0.5 \mu\text{M}$ (adjusted $R^2 = 0.98$) with a power coefficient of 3.7. DMSO = dimethylsulfoxide.

Table 1

Effects of V400M Mutation on Properties of Nav1.7

Parameter	Wild Type	V400M
V1/2 activation	$-43.9 \pm 1.5\text{mV}$	$-50.4 \pm 1.6\text{mV}$
k	4.3 ± 0.5	4.1 ± 0.4
V1/2 fast-inactivation	$-90.1 \pm 1.4\text{mV}$	$-82.8 \pm 1.4\text{mV}$
k	$6.8 \pm 0.3\text{mV}$	$6.5 \pm 0.3\text{mV}$
V1/2 slow-inactivation	$-73.9 \pm 3.9\text{mV}$	$-76.2 \pm 3.9\text{mV}$
k	12.4 ± 1.9	13.1 ± 2.7
Normalized slow-ramp peak	$0.95 \pm 0.11\%$ of peak current	$1.81 \pm 0.22\%$ of peak current
Voltage of slow-ramp peak	$-54.2 \pm 1.1\text{mV}$	$-63.1 \pm 2.4\text{mV}$

Table 2

Effects of Carbamazepine on Wild-Type and V400M Nav1.7

Treatment	V1/2 Activation		V1/2 Fast Inactivation	
	WT	V400M	WT	V400M
DMSO	-36.6mV	-47.9mV	-93.1mV	-87.2mV
0.3μM CBZ	-36.2mV	-47.8mV		
3μM CBZ	-37.4mV	-43.6mV		
10μM CBZ	-37.9mV	-36.9mV	-94.1mV	-91.7mV
30μM CBZ	-38.6mV	-36.1mV		
100μM CBZ	-40.5mV	-37.3mV	-94.7mV	-92.9mV

WT = wild type; DMSO = dimethylsulfoxide; CBZ = carbamazepine.